acta physica slovaca vol. 55 No. 5, 453 – 460 **October 2005**

PINK AFTERGLOW IN NITROGEN — HYDROCARBON MIXTURES[1]

F. Krčma[2]
Faculty of Chemistry, Brno University of Technology, Purkyňova 118, 612 00 Brno, Czech Republic

Received 18 April 2005, in final form 28 June 2005, accepted 8 July 2005

The effect of the nitrogen pink afterglow quenching by hydrocarbon traces is studied in the flowing afterglow regime. The Pyrex wall temperature around the observation point was varied between the ambient and liquid nitrogen temperature. The spectra of nitrogen N_2 1^{st} positive , N_2 2^{nd} pos. and N_2 1^{st} negative bands and CN violet and red systems were observed. The strong quenching of the vibrational populations of the nitrogen $N_2(B\,^3\Pi_g)$, $N_2(C\,^3\Pi_u)$ and $N_2^+(B\,^2\Sigma_u^+)$ states was observed and this effect increases with the decreasing wall temperature. The vibrational populations of $CN(A\,^2\Pi)$ and $CN(B\,^2\Sigma^+)$ states are more or less independent of the hydrocarbon concentration at the ambient wall temperature, but they increase with the decreasing temperature. A simplified kinetic model of the processes at our experimental conditions is presented, too.

PACS: 52.25.Vy, 52.25.Dg, 52.70.Kz

1 Introduction

The nitrogen post-discharges have been subjects of many studies for a relatively long time [1–5]. The relaxation processes of atomic and various metastable molecular states created during an active discharge lead to the common thermal equilibrium. Besides the collisional processes the light emission plays the significant role in the thermalization. Visible light can be observed up to one second after switching off the active discharge.

The first period (up to about 5 ms) of the post-discharge in the pure nitrogen is characterized by a strong decrease of the light emission. After that, the strong light emission at about 7–14 ms after the end of an active discharge is known as a pink afterglow and it can be observed in nitrogen only. It is manifested by a strong increase of the pink light emission at the decay times of about 8 ms in pure nitrogen and of about 28 ms in a nitrogen-argon mixture, while the yellow-orange colour is characteristic of the other parts of the nitrogen afterglow. The nitrogen pink afterglow can be characterized as a secondary discharge, because the electron concentration strongly increases due to various collisionally induced ionization processes [6,7] (see below) and

[1] Presented at Joint 15th Symposium on Applications of Plasma Processes (SAPP) and 3rd EU-Japan Symposium on Plasma Processing, Podbanské (Slovakia), 15 – 20 January 2005.

[2] E-mail address: krcma@fch.vutbr.cz

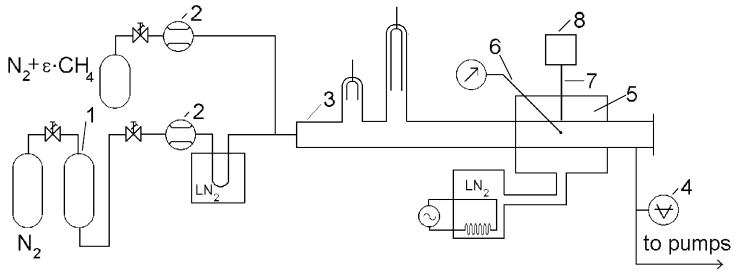

Fig. 1. A scheme of the experimental setup: 1. Catalyzer BASF R-3-11, 2. Mass flow controller, 3. Pyrex discharge tube, 4. Pirani gauge, 5. Cooled space, 6. Thermocouple, 7. Optical fiber, 8. Spectrometer.

thus the conditions are similar to those in the active discharge. The electron density measurements during the afterglow show the strong increase of the free electron concentration during this post-discharge period [8]. The effect of the nitrogen pink afterglow can be studied only in pure nitrogen, various traces (especially carbon and oxygen) quench it [9]. This work is focused on the pink afterglow quenching by hydrocarbon traces in the dependence on the temperature.

2 Experimental setup

The schematic drawing of our experimental arrangement is given in Fig. 1. We used the flowing system with a DC discharge (200 W) as an excitation source at the total gas pressure of 665 Pa. The nitrogen (purity of 99.999 %) had been further purified by a copper-based catalyzer and just before the rector tube by a liquid nitrogen trap. The hydrocarbon traces were injected into the pure nitrogen flow in their diluted form (100 ppm of hydrocarbon in the pure nitrogen) just before the active discharge. The spectra emitted during the afterglow in the range of 5 – 50 ms were measured by a Jobin Yvon HR 640 spectrometer with CCD. The discharge tube around the measuring point (in the range of $\pm$ 2.5 cm, i.e. $\pm$ 2.3 ms) can be cooled by liquid nitrogen vapor. This system allowed to vary the wall temperature in the range of 80 – 300 K that was measured by a thermocouple.

The relative vibrational populations were calculated using the Einstein coefficients and wavelengths given by Gilmore [10] and Prasad [11] from the following band head intensities:
for the $N_2(B\,^3\Pi_g)$ state from the $\triangle v$ = +6, +5, +4 and +2 sequencies,
for the $N_2(C\,^3\Pi_u)$ state from the $\triangle v$ = -2, -3 and -4 sequencies,
for the $N_2^+(B\,^2\Sigma_u^+)$ state from the $\triangle v$ = 0 and -1 sequencies.
for the $CN(A\,^2\Pi)$ state from the $\triangle v$ = +3 and +6 sequencies.
for the $CN(B\,^2\Sigma^+)$ state from the $\triangle v$ = 0 and -1 sequencies.
In the case when the band head was overlapped by another band, the population could not be calculated. The details of the other experimental conditions are described in [13].

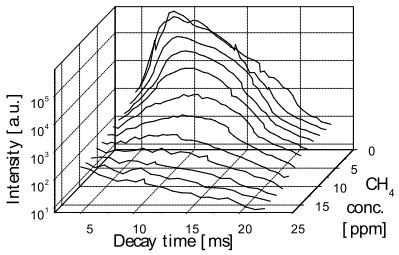

Fig. 2. N_2 1^{st} negative 0-0 band head intensity time profiles in relation to the methane concentration.

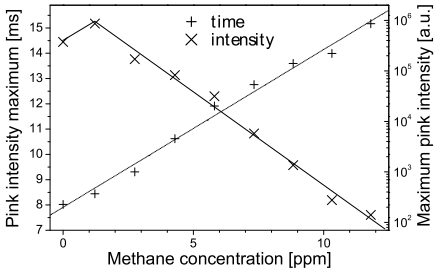

Fig. 3. Maximum intensity of the pink afterglow emission and its position as a function of methane concentration.

3 Results

The quenching of the nitrogen pink afterglow by the hydrocarbon traces of concentrations in the range of a few ppm was directly studied at the ambient temperature. The results of these observations were presented in the past in [9] and here they are only briefly summarized. The dependence of the nitrogen N_2 1^{st} negative 0-0 band head intensity (the main peak in the pink afterglow spectrum) is shown in Fig. 2 as a function of the decay time and the methane concentration. As it can be seen, the maximum of the pink afterglow intensity is decreasing with the methane concentration increase and the position of the maximum emission is also shifted to the later decay times. Both of these effects are linearly proportional to the methane concentration (See Fig. 3).

The vibrational distributions of $N_2(B\,^3\Pi_g)$ and $CN(A\,^2\Pi)$ states were studied as a function of the methane concentration at four wall temperatures between 77 K and 300 K at the decay time of 11 ms. The results are shown in Figs. 4 and 5. In the case of $N_2(B\,^3\Pi_g)$ state, the strong quenching of populations at all vibrational levels can be seen at methane concentrations accordingly to the observations in Fig. 2 and the effect is more evident at the ambient wall temperature. On the other hand, the vibrational populations of the $CN(A\,^2\Pi)$ state do not show any strong dependence on the methane concentration at the ambient wall temperature. When the wall temperature is decreased down to 77 K, the strong increase of the populations can be observed and the vibrational distribution is also dependent on the concentration.

The influence of hydrocarbon presence on the other observed spectral systems was studied at the same experimental conditions and only through the selected band due to the strong overlapping of these systems. The $N_2^+(B\,^2\Sigma_u^+)$ populations (resp. intensity of nitrogen N_2 1^{st} negative system) are strongly quenched by the methane presence accordingly to Fig. 2 at all wall temperatures. The quenching of $N_2(C\,^3\Pi_u)$ state populations is more or less the same as it was described for the $N_2(B\,^3\Pi_g)$ state. The $CN(B\,^2\Sigma^+)$ state (resp. intensity of the CN violet system) increases strongly with the increase of methane concentration. The increase is about 50 times higher when

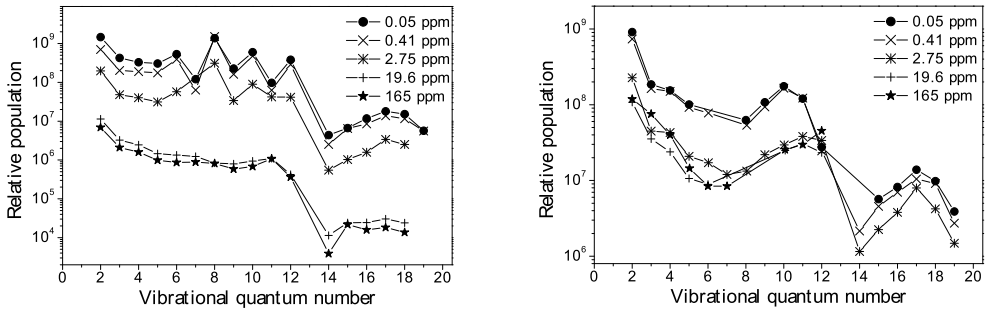

Fig. 4. Vibrational distributions of the $N_2(B\,^3\Pi_g)$ state as a function of the methane concentration at the decay time of 11 ms at the wall temperature of 300 K (left) and at 77 K (right).

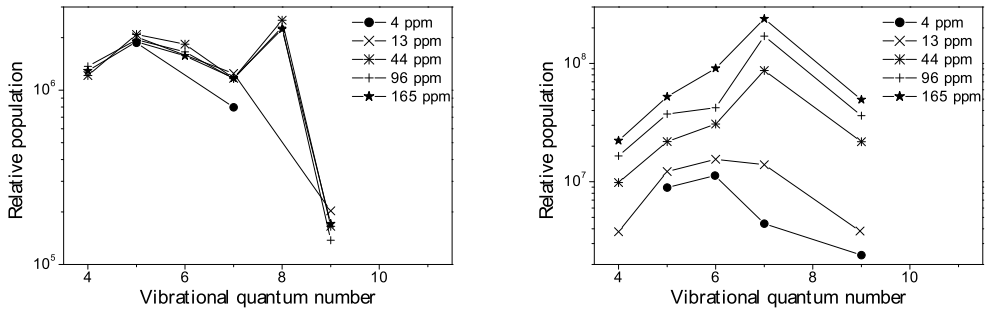

Fig. 5. Vibrational distributions of the $CN(A\,^2\Pi)$ state as a function of the methane concentration at the decay time of 11 ms at the wall temperature of 300 K (left) and at 77 K (right).

it was observed for the $CN(A\,^2\Pi)$ state (see Fig. 5). The same dependencies were also observed for all the studied molecular states when the partially or fully halogenated hydrocarbons were used [13].

4 Kinetic model

The nitrogen afterglow kinetics is a really complicated problem. The mechanisms that populate the radiative states of a neutral molecule and a molecular ion are different and they must be discussed separately.

4.1 Neutral nitrogen

The $N_2(B\,^3\Pi_g)$ and $N_2(C\,^3\Pi_u)$ states are dominantly created by pooling reactions of lower metastable states, especially by the vibrational excited ground state and by the lowest 8 levels

of $N_2(A\,^3\Sigma_u^+)$ state [2–4, 13]. These reactions show the creation of both these states, but they cannot explain the strong population enhancement during the pink afterglow. Therefore another process must be considered. It is known that in nitrogen post-discharge kinetics of the ground state the initial vibrational distribution changes by v-v process into the Treanor-Gordiets distribution that can be characterized by the significant enhancement of populations at higher vibrational levels. In the creation of the $N_2(B\,^3\Pi_g)$ and $N_2(C\,^3\Pi_u)$ states by pooling, the ground state must be excited at least to the levels of v = 4, resp. v = 19 when the pooling is with $N_2(A\,^3\Sigma_u^+)$ state or v = 14, resp. v = 24 when two ground states are involved. It is clear that at the end of an active discharge all these species are presented in the gas but their concentrations are much lower than the concentrations of the lowly excited molecules. The creation of higher vibrational levels takes some time, of course, and thus the dark space between the end of the active discharge and the pink afterglow can be observed. The pooling reactions can also lead to creation of the $N_2(A\,^3\Sigma_u^+)$ state, and thus the pink afterglow effect is further enhanced. The reaction scheme can be written as follows (for references and rate constants see [14]):

$$N_2(X\,^1\Sigma_g^+, v) + N_2(X\,^1\Sigma_g^+, w) \rightarrow N_2(X\,^1\Sigma_g^+, v+1) + N_2(X\,^1\Sigma_g^+, w-1) \quad (1)$$

$$2N_2(X\,^1\Sigma_g^+, v \geq 12) \rightarrow N_2(A\,^3\Sigma_u^+) + N_2 \quad (2)$$

$$N_2(X\,^1\Sigma_g^+, v \geq 25) + N(^4S^0) \rightarrow N_2(A\,^3\Sigma_u^+) + N(^4S^0) \quad (3)$$

$$N_2(X\,^1\Sigma_g^+, v \geq 25) + e \rightarrow N_2(A\,^3\Sigma_u^+) + e \quad (4)$$

$$N_2(X\,^1\Sigma_g^+, v \geq 35) + N(^4S^0) \rightarrow N_2(a\,^1\Pi_g) \text{ or } N_2(a\prime\,^1\Sigma_u^-) + N(^4S^0) \quad (5)$$

$$N_2(X\,^1\Sigma_g^+, v \geq 35) + e \rightarrow N_2(a\,^1\Pi_g) \text{ or } N_2(a\prime\,^1\Sigma_u^-) + e \quad (6)$$

$$2N_2(X\,^1\Sigma_g^+, v \geq 14) \rightarrow N_2(B\,^3\Pi_g) + N_2 \quad (7)$$

$$N_2(X\,^1\Sigma_g^+, v \geq 4) + N_2(A\,^3\Sigma_u^+, v) \rightarrow N_2(B\,^3\Pi_g) + N_2 \quad (8)$$

$$2N_2(A\,^3\Sigma_u^+) \rightarrow N_2(B\,^3\Pi_g) + N_2 \quad (9)$$

$$2N_2(X\,^1\Sigma_g^+, v \geq 24) \rightarrow N_2(X\,^1\Sigma_g^+) + N_2(C\,^3\Pi_u) \quad (10)$$

$$N_2(X\,^1\Sigma_g^+, v \geq 19) + N_2(A\,^3\Sigma_u^+) \rightarrow N_2 + N_2(C\,^3\Pi_u) \quad (11)$$

$$2N_2(A\,^3\Sigma_u^+) \rightarrow N_2(X\,^1\Sigma_g^+) + N_2(C\,^3\Pi_u) \quad (12)$$

$$N_2(A\,^3\Sigma_u^+) + N_2(B\,^3\Pi_g) \rightarrow N_2(X\,^1\Sigma_g^+) + N_2(C\,^3\Pi_u) \quad (13)$$

The first six reactions form the precursors, the other lead to the formation of both radiative states. The reaction 1 is well known as v-v pumping process and plays the significant role during the whole nitrogen afterglow. Also the reaction 2 is running about all the time without any significant changes. The reactions 3 – 6 are probably the most important for the pink afterglow creation. They need highly vibrationally excited ground state molecules that are not presented during the afterglow beginning in higher concentrations and they must be created by v-v process (reaction 1). This takes a some time and thereafter the electronicaly excited molecules are created and consequently they can react with molecules excited to the lower vibrational levels. This mechanism can explain the lower radiative afterglow part between the active discharge and the pink afterglow. The other metastable states, especially metastable singlet states, must be of course included in the scheme, when a numeric modeling will be used. This simplified reaction scheme clearly demonstrates the main principles of the pink afterglow creation. Much more complex description of the mechanisms was described recently in [15, 16].

4.2 Nitrogen molecular ion

The kinetics of the molecular ion radiative state is more complicated and it can be explained in a two-step scheme. Before the pink afterglow the charged particles concentration is very low [8] but during the pink afterglow it significantly increases. So, the first step must lead to the molecular ion creation. Due to the fact that the post-discharge is without any external energy source, some of the kinetic processes must be efficient enough for the ionization. The whole process is known as a step-wise ionization [6, 7]. In its principle, the highly excited neutral metastable molecules (excited both electronically and vibrationally) can have energy sufficient for the ionization during their collisions. Precursors for the ionizing collisions are created by the process (1) and by processes similar to (2). When the molecular ion is created, the excitation to the radiative state must be completed. Recent studies have demonstrated that the main process responsible for the population of the radiative $N_2^+(B\,^2\Sigma_u^+)$ state is the collisionally induced energy transfer from the vibrationally excited neutral ground state [13]. The reactions describing kinetics of the molecular ion are, besides the reaction (1), as follows:

$$N_2(X\,^1\Sigma_g^+, v) + N_2(X\,^1\Sigma_g^+, w) \rightarrow N_2^* + N_2 \tag{14}$$

$$2N_2(X\,^1\Sigma_g^+, v \geq 32) \rightarrow N_2^+(B\,^2\Sigma_u^+) + N_2 + e \tag{15}$$

$$N_2(X\,^1\Sigma_g^+, v) + N_2^* \rightarrow N_2^+ + N_2 + e \tag{16}$$

$$N_2^* + N_2^* \rightarrow N_2^+ + N_2 + e \tag{17}$$

$$N_2(X\,^1\Sigma_g^+, v \geq 12) + N_2^+(X\,^2\Sigma_g^+) \rightarrow N_2(X\,^1\Sigma_g^+) + N_2^+(B\,^2\Sigma_u^+) \tag{18}$$

The N_2^* in the reactions above means an electronically excited metastable neutral molecule, especially $N_2(A\,^3\Sigma_u^+)$, $N_2(a\,^1\Pi_g)$ and $N_2(a\prime\,^1\Sigma_u^-)$) states.

4.3 CN radical

The CN radical kinetics can be described in a simplified form by the following scheme:

$$N(^4S^0) + C(^3P) + M \rightarrow CN + M \tag{19}$$

$$N_2^* + CN \rightarrow N_2 + C + N \tag{20}$$

$$N_2(X\,^1\Sigma_g^+, v \geq 4) + CN(X\,^2\Sigma) \rightarrow N_2(X\,^1\Sigma_g^+) + CN(A\,^2\Pi) \tag{21}$$

$$N_2(X\,^1\Sigma_g^+, v \geq 12) + CN(X\,^2\Sigma) \rightarrow N_2(X\,^1\Sigma_g^+) + CN(B\,^2\Sigma^+) \tag{22}$$

Reaction 19 represents the CN radical formation by three body recombination (M means a third body, in our case it isdominantly nitrogen neutral molecule or the reactor wall). The other two processes are nearly resonant [13, 17] and due to the high concentration of the vibrationally excited neutral nitrogen ground state they are very effective sources for the strong CN spectra emission.

The reactions 21 and 22 play a significant role in the v-v process described by the reaction 1. Due to the fact that the excited states of the CN radical are radiative, the reactions 21 and 22 can be repeated many times, and thus the v-v process could not effectively populate the higher vibrational levels needed for the creation of all higher states. Moreover, the reaction 20 effectively

decreases the concentration of the electronically excited nitrogen states. Thus the $N_2(B\,^3\Pi_g)$, $N_2(C\,^3\Pi_u)$ and N_2^+ species could not be formed as effectively as in pure nitrogen and the pink afterglow is quenched. The presented simplified kinetic model could not explain all the processes and more experimental and theoretical studies must be further carried on.

The specific problem is the influence of the wall temperature. When the temperature decreases the wall collisions change their rate constants. These effects were not been yet studied directly and thus it is difficult to include them correctly. The situation is rather better for the volume processes. The collisions become more non-elastic and they are also more selective because the rotational excitation is much lower then at the ambient temperature. Also it is known that some reactions, for example three body recombination, have negative temperature dependence of their rate coefficients. The explanation of the experimental results presented in Figs. 4 and 5 is thus very complicated and more experiments will be needed. The first of them will be caried out using the quatz discharge tube to verify the wall collisions influence because the wall processes play the significant role in the nitrogen post-discharge kinetics.

5 Conclusion

The nitrogen pink afterglow was studied in the flowing regime as a function of the wall temperature and the hydrocarbon concentration. The vibrational distributions of the neutral molecule radiative states as well as the nitrogen molecular ion radiative $N_2^+(B\,^2\Sigma_u^+)$ state show the strong quenching of the populations during the pink afterglow when the hydrocarbon traces are added into the pure nitrogen. This effect increases when the wall temperature around the observation point is decreased down to the liquid nitrogen temperature. The CN radical vibrational distributions are more or less independent of the hydrocarbon concentration at the ambient wall temperature, but all the populations significantly increase with the decreasing temperature. The presented kinetic model demonstrates the dominant role of the highly vibrationally excited neutral nitrogen ground state in the post-discharge kinetics of the nitrogen states. The role of the CN radical created during the active discharge and the post-discharge is dominant in the blocking of the v-v processes that are the main sources for the creation of the highly excited nitrogen states (including the creation of a molecular ion) in the post-discharge period. The presented simplified kinetic model could not explain all the observed processes and more experimental and theoretical studies must be further carried on. Especially the other nitrogen metastable states must be included in these studies.

Acknowledgement: This work was supported by the Czech Science Foundation, contracts No. 202/98/P258 and 202/05/0111.

References

[1] G. E. Beale, H. P. Broida: *J. Chem. Phys.* **31** (1959) 1030
[2] L. G. Piper: *J. Chem. Phys.* **88** (1988) 231
[3] L. G. Piper: *J. Chem. Phys.* **88** (1988) 6911
[4] L. G. Piper: *J. Chem. Phys.* **91** (1989) 864
[5] V. Guerra, P. A. Sa, J. Loureiro: *J. Phys. D, Appl. Phys.* **34** (2001) 1745
[6] L. S. Polak, D. I. Sloveckii, A. S. Sokolov: *Opt. Spectrosc.* **32** (1972) 247

[7] F. Paniccia, C. Gorse, M. Cacciatore, M. Capitelli: *J. Appl. Phys.* **61** (1987) 3123
[8] J. Janča, A. Tálský, N. El Kattan: *Folia Physica* **27** (1978) 23
[9] F. Krčma, L. Babák: *Czech. J. Phys.* **49** (1999) 271
[10] F. R. Gilmore, R. R. Laher, P. J. Espy: *J. Phys. Chem. Ref. Data* **21** (1992) 1005
[11] C. V. V. Prasad, P. F. Bernath, C. Frum, R. Engelman: *J. Mol. Spectrosc.* **151** (1992) 459
[12] C. V. V. Prasad, P. F. Bernath: *J. Mol. Spectrosc.* **156** (1992) 327
[13] F. Krčma, E. T. Protasevich: *Post-discharges in Pure Nitrogen and in Nitrogen Containing Halogenated Hydrocarbon Traces, Tomsk Polytechnic University Publishing, Tomsk 2003*
[14] F. Krčma: *http://www.fch.vutbr.cz/home/krcma/publications/95-thesis-appendix1.pdf*
[15] N. Sadeghi, C. Foissac, P. Supiot: *J. Phys. D, Appl. Phys.* **34** (2001) 1779
[16] P. A. Sa, V. Guerra, J. Loureiro, N. Sadeghi: *J. Phys. D, Appl. Phys.* **37** (2004) 221
[17] J. Hubeňák, F. Krčma: *J. Phys. D, Appl. Phys.* **33** (2000) 3121